

RESEARCH PAPER



Artemisinin displays bactericidal activity via copper-mediated DNA damage

In-Young Chung, Hye-Jeong Jang, Yeon-Ji Yoo, Joonseong Hur, Hyo-Young Oh, Seok-Ho Kim, and You-Hee Cho 

Department of Pharmacy, College of Pharmacy and Institute of Pharmaceutical Sciences, Cha University, Gyeonggi-do, Korea

ABSTRACT

Artemisinin (ARS) and its semi-synthetic derivatives are effective drugs to treat malaria and possess multiple therapeutic activities based on their endoperoxide bridge. Here, we showed that ARS displayed antibacterial efficacy in *Drosophila* systemic infections caused by bacterial pathogens but killed only *Vibrio cholerae* (VC) in vitro, involving reactive oxygen species (ROS) generation and/or DNA damage. This selective antibacterial activity of ARS was attributed to the higher intracellular copper levels in VC, in that the antibacterial activity was observed in vitro upon addition of cuprous ions even against other bacteria and was compromised by the copper-specific chelators neocuproine (NC) and triethylenetetramine (TETA) in vitro and in vivo. We suggest that copper can enhance or reinforce the therapeutic activities of ARS to be repurposed as an antibacterial drug for the treatment of bacterial infections.

ARTICLE HISTORY

Received 18 February 2021
Revised 13 December 2021
Accepted 16 December 2021

KEYWORDS

Artemisinin; antimalarial; antibacterial; copper; *Vibrio cholerae*

Introduction

Antimicrobial resistance (AMR) of bacterial pathogens is a growing problem worldwide [1]. The emergence of pathogens resistant to one or more antimicrobial drugs is increasing at an alarming rate. As a result, infectious diseases that are extremely difficult or impossible to treat with conventional drugs are becoming a global health threat. A critical component of the AMR solution is the development of novel antimicrobial drugs to cover the diminishing effectiveness of the currently available antibacterial regimens. Although conventional antibiotic pipelines need to be substantially reinvigorated in response to the growing emergency, much attention has been recently paid to drug repurposing or repositioning that utilizes approved drugs or abandoned compounds to treat a different indication [2]. This approach is valid in that known drugs and compounds have already been tested in humans and detailed information is available regarding their pharmacology, formulation, dose, and toxicity, etc., [3]. This “salvage” discovery either via the established mechanism of action or by identification of new ones is advantageous over traditional “de novo” discovery in that it could significantly reduce the discovery and development timeline as well as the overall cost of bringing drugs to market.

ARS is the most potent antimalarial drug obtained from the extract of *Artemisia annua* [4,5]. It is widely

used not only for the rapid treatment of *Plasmodium falciparum* malaria but also for its high safety with few side effects and its tolerance profile [6,7]. ARS is a sesquiterpene lactone-type compound, and its pharmacophore is considered to be the endoperoxide bridge of its 1,2,4-trioxane moiety [8]. Based on the pharmacophore of ARS, several semi-synthetic derivatives have also been developed for effective clinical use, including artesunate, arteether, and artemether [9,10]. Multiple antimalarial mechanisms of ARS have been suggested and have yet to be fully understood. Nevertheless, the generation of reactive oxygen species (ROS) via endoperoxide bridge cleavage of the 1,2,4-trioxane scaffold is the presumable cytotoxic mechanism of ARS [11,12]. Furthermore, previous studies demonstrated that the decomposition of ARS was induced by hemes or free ferrous ion, which is mediated by a Fenton reaction [12,13]. Besides ferrous iron, cuprous copper could also catalyze the reductive activation of ARS at the endoperoxide in vitro [14]. The ARS-derived ROS and/or the carbon-centered organic radicals have the potential to facilitate the clearance of the parasite *P. falciparum* from the blood [11,15]. The ability of ARS carbon-centered radicals to alkylate hemes and specific proteins in the parasite has been suggested to be the key to the antimalarial activity [16–18]. Two parasite proteins, the translationally

CONTACT You-Hee Cho  youhee@cha.ac.kr

 Supplemental data for this article can be accessed [here](#)

controlled tumor protein homolog and the sarcoplasmic reticulum Ca^{2+} -transporting ATPase of *P. falciparum* (identified as PfATP6), have been reported as the putative targets of ARS, but the current consensus is that PfATP6 is not directly involved in the action or resistance of ARS [19,20]. Although the exact molecular mechanism of targeting and inhibition by ARS has yet to be discovered, it is clear that its antimalarial activity is dependent on transition metals, such as iron [21].

Beyond its antimalarial activity, ARS and its derivatives have been shown to possess multiple therapeutic activities, such as antiviral, antifungal, anticancer, and anti-inflammatory activities [22–26]. These activities might also involve ROS generation, which has been verified to cause cellular damage. Since ROS generation is also implicated in antibacterial mechanisms for bactericidal antibiotics and redox-cycling chemicals, it would be worthwhile to explore the potential antibacterial activity of ARS, based on its generation of ROS in the presence of iron or other transition metals.

In this study, we have confirmed the antibacterial activity of ARS by enhancing its solubility and by improving the intrinsic antibacterial activity [27]. As a result, we have identified a previously unexplored bactericidal activity of ARS in the presence of a transition metal ion, Cu^+ , which enhances the antibacterial activity of ARS in vitro. All the tested bacteria were permeable to ARS, but the MIC values differed markedly, with the lowest (3.13 $\mu\text{g}/\text{ml}$) for VC. We also observed that ROS generation and/or DNA damage might be the key to the bactericidal activity of ARS as previously reported for the antimalarial activity [28]. These results suggest that ARS could be repurposed as an antibacterial against VC.

Materials and methods

Bacterial strains and culture conditions

The bacterial strains used in this study are listed in Table S1. PA, VC, EC, SA, and BS strains were grown at 37°C using Luria-Bertani (LB) (1% tryptone, 0.5% yeast extract, and 1% NaCl) broth, Müller-Hinton (MH) broth (Cat No. 275,730; BD Difco, USA), and M9-glucose minimal medium (1.2% Na_2HPO_4 , 0.3% KH_2PO_4 , 0.05% NaCl, 0.1% NH_4Cl , 2 mM MgSO_4 , 0.1 mM CaCl_2 , and 0.4% glucose) or on 2% Bacto agar-solidified LB plates. Overnight-grown cultures were used as inoculum (1.6×10^7 cfu/ml) into fresh medium and grown at 37°C in a shaking incubator up to the logarithmic ($\text{OD}_{600} = 0.7$) phase, and then the cell cultures were used for the experiments described herein.

ARS and its derivatives

ARSF, which is conjugated with an acridine moiety, was synthesized and purified as described previously [20]. ARS and ART were purchased from Sigma-Aldrich (Cat No. 361,593 and A3731; USA). The other ARS derivatives (compounds 3–10) were obtained from Toronto Research Chemicals (Cat No. A777400, A774300, D448360, A637875, A777550, D294728, A794900, and D232150; Canada). The compounds were dissolved in dimethyl sulfoxide (DMSO).

Assessment of permeability

The bacterial cells were cultured to OD_{600} of 0.7 in LB medium. The cell cultures were incubated with 0.1 mg/ml of ARSF for 5 min and 40 min. After incubation, the cells were washed with PBS buffer (10 mM Na_2HPO_4 , 1.8 mM KH_2PO_4 , 137 mM NaCl, 2.7 mM KCl; pH 7.4) twice. The penetrated ARSF was detected by using an Axio 5 fluorescence microscope (Carl Zeiss, Germany) at 488-nm excitation.

Measurement of antibacterial efficacy

Drosophila systemic infection was performed as previously described [29,30]. *Drosophila melanogaster* strain Oregon R, was grown and maintained at 25°C using corn meal-dextrose medium [0.93% agar, 6.24% dry yeast, 4.08% corn meal, 8.62% dextrose, 0.1% methyl paraben, and 0.45% (v/v) propionic acid]. For systemic infection, 4- to 5-day-old adult female flies were infected by pricking at the dorsal thorax with a 0.4 mm needle (Ernest F. Fullam, Inc., USA). The needle was dipped into PBS-diluted bacterial suspension containing PA (10^7 cfu/ml), VC (5×10^7 cfu/ml) or SA (10^8 cfu/ml) grown to the OD_{600} of 3.0. Prior to infection, the flies were pretreated with a new medium overlaid with 50 μl of ART (0.1, 0.5, 1 or 5 mg/ml) for 18 h. Infected flies were transferred to the medium overlaid with ART. For copper-chelation, media overlaid with 50 μl of ART (1 mg/ml) and 50 μl of NC (1 or 10 μM) (Cat No. N1501; Sigma-Aldrich, USA) were prepared. Survival rates of the infected flies were monitored for up to 72 h post-infection. Flies that died within 12 h for PA and SA, 6 h for VC were excluded in mortality determination. Each mortality assay was repeated at least four times.

Measurement of antibacterial activity

The antibacterial activity was evaluated by spotting assay, LIVE/DEAD BacLight staining (Cat No. L7007;

Invitrogen, USA), and viability assay. For transition metal treatment, sub-lethal concentrations (1/2 or 1/4 MIC) of FeSO₄ (Cat No. 215,422; Sigma-Aldrich, USA) and CuCl (Cat No. 229,628; Sigma-Aldrich, USA) were added to LB or MH media.

Spotting assay

The bacterial cells were cultured to OD₆₀₀ of 0.7 in LB medium. Ten-fold serial dilutions (3 µl) of the cell cultures in LB broth were spotted onto an LB agar plate containing ARS and its derivatives to enumerate the surviving bacteria. The plates were incubated overnight at 37°C.

LIVE/DEAD BacLight staining.

The bacteria were cultured to OD₆₀₀ of 0.7 in LB broth and then diluted to approximately 10⁷ cfu/ml. The cells were treated with ART and/or CuCl for 1 h. After the treatment, the cells were stained with 6 µM SYTO9 and 30 µM propidium iodide (PI) for 15 min at room temperature. The stained cells were observed by using an Axio 5 fluorescence microscope (Carl Zeiss, Germany) at 480-nm excitation for SYTO9 and at 490-nm excitation for PI.

Viability assay

The indicated bacterial strains (1 × 10⁸ cfu/ml) that had been grown to the logarithmic growth phase (OD₆₀₀ = 0.7) were treated with a sub-lethal concentration (1/4 MIC) of ART for 5 h. The colony forming units were measured.

Copper chelation and detection

For copper chelation, the cells were pretreated with either NC (1.5 µM) or TETA (1.5 mM) (Cat No. 259,535; Sigma-Aldrich, USA) for 2 h before ART or H₂O₂ treatment. To qualitatively measure the intracellular level of copper ions, the bacteria were cultured to OD₆₀₀ of 0.7 in LB broth containing 10 µM of CuCl. The cells were then washed and incubated in 10 µM of CopperGREENTM (Cat No. GC902; Goryo Chemical, Japan), which is known to selectively react with Cu⁺ for 1 h. The intracellular level of Cu⁺ was visualized under a fluorescence microscope.

Determination of minimal inhibitory concentrations (MICs)

MICs for ARS and its derivatives were determined in MH broth by the broth microdilution method using standard microbiological procedures according to NCCLS guidelines, as per document no. M07-A8

(2012) [31]. The medium with a 2-fold serial dilution of each compound in MH broth was subjected to inoculation with the indicated bacterial strains (5 × 10⁵ cfu/ml) that had been grown at 37°C to the logarithmic growth phase (OD₆₀₀ = 1.0) and then incubated at 37°C on a rotary shaker. The MIC values were recorded to be the lowest concentration of the compound at which no signs of growth were observed based on the OD₆₀₀ value of less than 0.05 after 18 h of incubation.

Measurement of ROS generation

ROS generation was detected using hydroxyphenyl fluorescein (HPF) (Cat No. H36004; Invitrogen, USA), which is known to react with hydroxyl radicals and peroxy nitrite anions. The bacteria were cultured to OD₆₀₀ of 0.5 in M9 minimal medium and incubated with HPF (5 µM) for 30 min. The cells were then washed and resuspended in 1 ml of M9 minimal medium containing 313 µg/ml of ARS. The samples were incubated for 3 h at 37°C, and the fluorescence was imaged using an LSM 880 scanning confocal microscope (Carl Zeiss, Germany) at 488-nm excitation.

Measurement of DNA damage

DNA damage was evaluated in vivo by detection of RecN foci, and in vitro by DNA strand break assay.

Detection of RecN foci

The *recN* gene was fused with mClover3 at N-terminus with a linker (GLGSGGGSGGGSGGTA) and then cloned into pBAD24, which was introduced into the wild type VC. The bacteria were grown to an early logarithmic growth phase (OD₆₀₀ = 0.3) with 0.2% arabinose. The cells (1 µl) were applied on 2% agarose pads containing either AT (31.3 µg/ml) and H₂O₂ (150 µM), and incubated for 30 min. The dsDNA break foci were monitored using an Axio 5 fluorescence microscope (Carl Zeiss, Germany) at 488-nm excitation.

DNA strand break assay

For the DNA strand break assay, the conversion of plasmid from supercoiled form to open circular form was detected as previously described [32]. 30 ng of the pUCP19 plasmid was incubated in a 3.5 mM NaHCO₃ buffer (pH 7.2) with 20 µM glutathione (GSH) (Cat No. PHR1359; Sigma-Aldrich, USA) as a reductant to recycle the metal ions, 10 mM ARS or ART, and 10 µM FeSO₄ or CuCl for 20 min. The reaction mixture was resolved by electrophoresis on a 1% agarose gel, and then visualized with UV light after EtBr staining.

Time-to-kill experiment

The bacteria were cultured to OD₆₀₀ of 0.7 in MH broth and then diluted to approximately 5×10^5 cfu/ml. The cell cultures were treated with 1.56, 3.13, 6.25, and 12.5 µg/ml of ARS and incubated at 37°C. At 1- or 2-h time intervals, aliquots (1 ml) were taken from the samples and then plated onto MH agar plates to enumerate viable bacteria. The experiments were performed four times.

Statistics

Statistical analysis was performed using GraphPad Prism version 8.0 (GraphPad Software, USA). Data for each analysis represent a set of three repetitions. Statistical significance between the groups is indicated, based on a *p* value of less than 0.01 (*, *p* < 0.01; **, *p* < 0.005, ***, *p* < 0.001) by using the Kaplan–Meier log-rank test and Student's *t* test. Error bars represent standard deviation.

RESULTS

ARS is permeable to bacterial species

To investigate the potential antibacterial activity of ARS, especially against Gram-negative bacteria, we initially tested the permeability to ARS of bacterial cells by using an acridine-linked fluorescent ARS derivative (ARSF) (Figure S1A) [20]. The bioactivity of ARSF was not affected at all by the covalent conjugation with the fluorescent moiety (Figure S1B). As shown in Figure 1, ARSF-derived green fluorescence was distributed in the cytoplasm of the budding yeast,

Saccharomyces cerevisiae (SC), which is reported to be susceptible to ARS [33]. Fluorescence was also detected inside the tested Gram-negative and Gram-positive bacteria within 5 min after ARSF treatment, suggesting that ARSF rapidly penetrated the bacterial cell membrane, especially in VC, *Staphylococcus aureus* (SA), and *Bacillus subtilis* (BS). More interestingly, the ARSF-derived fluorescence remained for several minutes, except in the VC cells, where the fluorescence formed foci within 40 min.

ARS displays antibacterial activity in *Drosophila* infection

To assess the potential antibacterial activity of ARS, we first exploited the *Drosophila* systemic infection model established for the major bacterial pathogens, which is amenable to elucidating the antibacterial efficacy of candidate compounds [30,34]. We tested artesunate (ART), which displays better aqueous solubility than ARS and thus is more appropriate for the *Drosophila* infection model. The flies were pricked with PA, VC, or methicillin-resistant SA as described in Materials and Methods. ART (0.1–5 mg/ml) was included in the fly media for feeding the flies 18 h prior to infection. Figure 2 shows that ART rescued the infected flies from mortality caused by PA or SA at 1 or 5 mg/ml and interestingly by VC even at 0.1 or 0.5 mg/ml (Figure 2(c)). These protective effects of ART against both Gram-negative and Gram-positive bacterial pathogens, especially VC, have led us to the idea of repurposing ARS and its derivatives to antibacterial drugs.

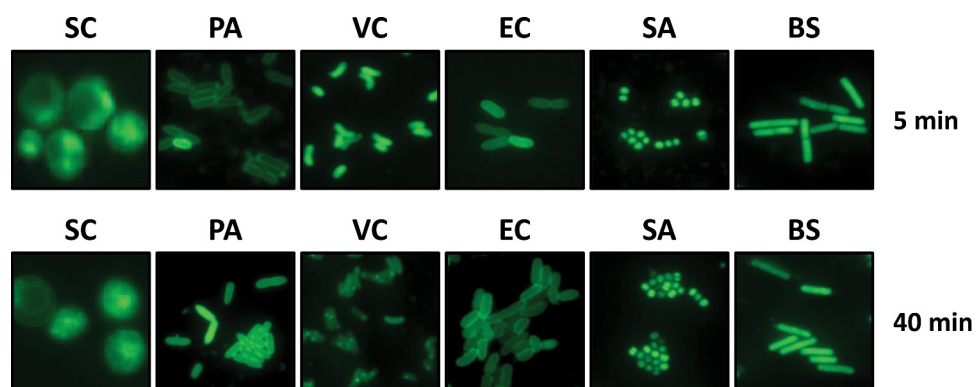


Figure 1. Permeability of ARS in bacterial species.

Representative fluorescence microscopic images by fluorescence-labeled ARS (ARSF) in yeast and various bacterial species. The budding yeast (*S. cerevisiae*, SC) and Gram-negative (*P. aeruginosa*, PA; *V. cholerae*, VC; and *E. coli*, EC) and Gram-positive (*S. aureus*, SA; and *B. subtilis*, BS) bacteria were incubated with 0.1 mg/ml of ARSF for 5 min (upper panel) and 40 min (lower panel). After incubation, the cells were washed with PBS, and visualized by fluorescence microscopy. No autofluorescence was detected without ARSF in this experimental condition.

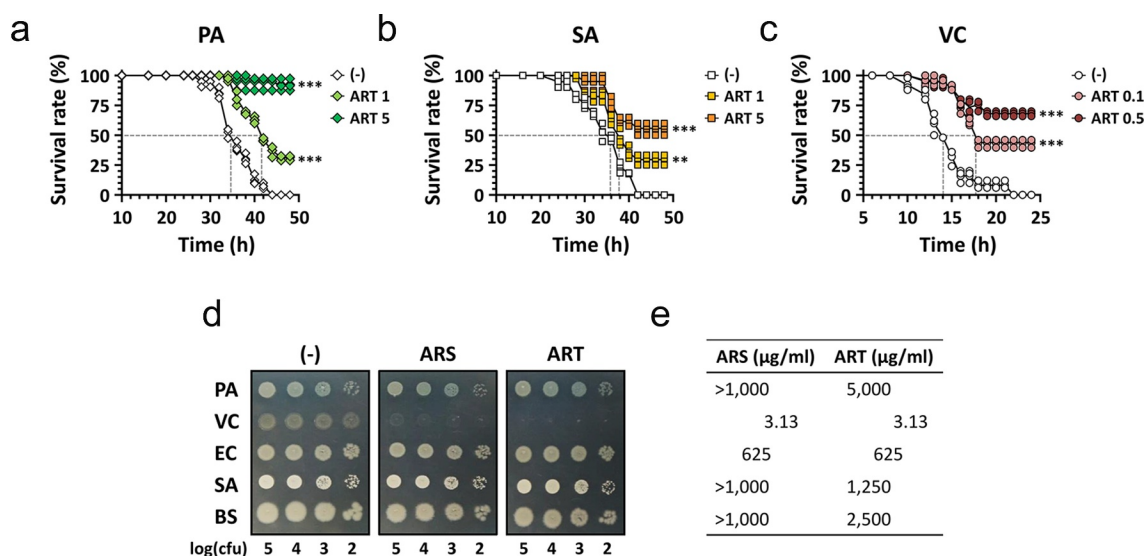


Figure 2. Antibacterial efficacy of ARS in vivo and in vitro.

(A to C) Survival rates of bacteria-infected flies were determined upon administration of an ARS derivative, artesunate (ART). The bacterial pathogens such as PA (A), SA (B), and VC (C) were introduced into the flies with either nothing (open) or ART (1 mg/ml or 5 mg/ml for PA and SA, 0.1 mg/ml or 0.5 mg/ml for VC) (filled). Those infected flies were transferred to the new corn meal media, and the survival was measured over time. The dotted lines represent the time required to reach 50% mortality. The statistical significance based on a log-rank test is indicated (**, $p < 0.005$; ***, $p < 0.001$). (D) Susceptibility of bacterial species to ARS and ART. The Gram-negative (PA, VC, and EC) and Gram-positive (SA and BS) cells were grown to a logarithmic growth phase. Ten-fold serial dilutions from the cell cultures were spotted onto an LB agar plate (-) or an LB agar plate containing 12.5 $\mu\text{g/ml}$ of either ARS or ART. The numbers indicate the $\log(\text{cfu})$ of the applied bacterial spots. (E) Minimal inhibitory concentrations (MICs) of ARS and ART for the bacterial species in (D).

ARS displays antibacterial activity in vitro against VC

To further investigate ARS for antibacterial use, we assessed its in vitro antibacterial activity. Unexpectedly, this activity was not fully consistent with the in vivo antibacterial efficacy against the bacterial pathogens. The test revealed that only VC was susceptible to ARS treatment (Figure 2(d)). VC cells in the logarithmic growth phase rarely survived, as the number of cells was reduced by more than 10^5 fold on LB agar plates with ARS or ART, whereas the other bacteria were not susceptible. The MICs of ARS were also determined for the bacterial pathogens (Figure 2(e)); the lowest value of 3.13 $\mu\text{g/ml}$ (12.5 mM) was obtained for VC, a value 200- to 1,000-fold less than those for the other bacteria. These results suggest that the antibacterial activity of ARS has rarely been observed in vitro against the bacterial pathogens except for VC under ordinary experimental conditions.

A variety of the semi-synthetic ARS derivatives have been developed to study the structure–activity relationship (SAR) of the ARS bioactivity [35]. We have tested nine ARS derivatives for antibacterial activity using VC (Figure S2). Dihydroartemisinin (compound 5) was the most effective at killing VC, with an MIC value of less than 1.56 $\mu\text{g/ml}$. Deoxyartemisinin (compound 10), which does not possess

the endoperoxide, was not effective at all (i.e. MIC > 100), indicating the importance of the endoperoxide bridge in VC killing as for antimalarial activity [8]. The other derivatives used in this study displayed no less antibacterial activity than did ARS, except for 9-desmethylene 9-oxo-artemisinin (compound 8). This suggests the critical involvement of the hydrophobic substituents at the C11 position of the ARS scaffold in VC killing.

ARS is associated with reactive oxygen species (ROS) formation and DNA damage

Previous studies have suggested that ARS-mediated ROS generation contributes to the antimalarial activity [11,15]. To assess whether the ART treatment resulted in ROS formation in VC, the increase in the intracellular ROS level was assessed after ART treatment. Intracellular ROS was observed by staining with hydroxyphenyl fluorescein (HPF), which is known to sense hydroxyl radicals. As shown in Figure 3(a), ART treatment led to elevated fluorescence, indicative of ROS formation in VC, in contrast to no sign of ROS formation in ARS-resistant bacteria (PA and EC). To further confirm that ROS formation plays a role in the ART antibacterial activity against VC, we examined the ART-mediated growth inhibition of VC

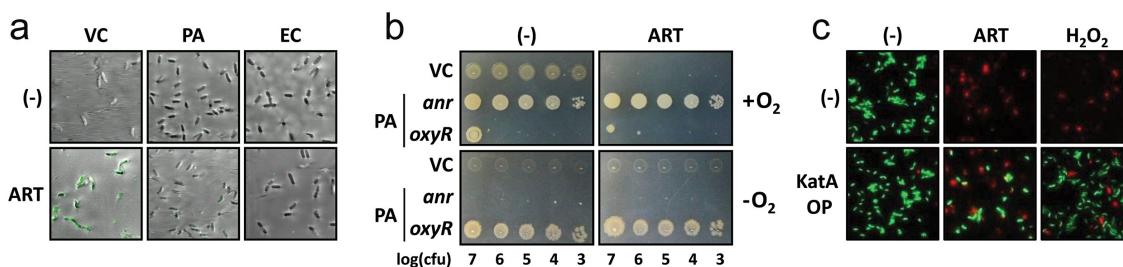


Figure 3. Enhancement of ARS-induced ROS generation in VC.

(A) ROS generation by ART in vivo. The VC, PA, and EC cells (5×10^5 cfu/ml) that had been grown to a logarithmic growth phase were incubated for 3 h in M9 minimal medium containing hydroxyphenyl fluorescein (HPF), with nothing (-) or ART (313 μ g/ml). The ROS generation is analyzed by the levels of the HPF fluorescence under fluorescence microscope, which were merged with the bright-field microscopic images. (B) Antibacterial activity of ART under anaerobic condition. The VC and PA (*anr* and *oxyR* mutants) cells were grown to the logarithmic growth phase. Ten-fold serial dilutions from the cell cultures were spotted onto an LB agar plate (-) or an LB agar plate containing 12.5 μ g/ml of ART for aerobic culture. For anaerobic culture, 50 mM KNO_3 was added to LB agar plates. The numbers indicate the log(cfu) of the applied bacterial spots. (C) Effect of catalase on ARS-induced VC killing. The VC cells containing either pBAD24 (-) or pBAD24-KatA (KatA OP) were grown to the logarithmic growth phase and then pulse-treated with ART (313 μ g/ml) or H_2O_2 (750 μ M). After treatment, the cells were stained using the mixture of SYTO9 and propidium iodide (PI) and visualized by fluorescence microscope.

under anaerobic conditions (Figure 3(b)). The *oxyR* and *anr* mutants of PA were included to monitor the anaerobic culture condition, in that anaerobic conditions do support the serial dilution of the PA *oxyR* mutant, but not that of the PA *anr* mutant [36,37]. As a result, the antibacterial activity was not clearly observed under anaerobic conditions, despite the fact that growth and the colony morphotypes have apparently been altered under the anaerobic conditions. We also confirmed that the ART-mediated VC killing was abrogated by ectopic expression of a stable catalase from PA (KatA) [38], as assessed by the LIVE/DEAD BacLight viability probe (Figure 3(c) and S3). Given that KatA efficiently removes the toxic amount of H_2O_2 , a relatively stable intermediate ROS during aberrant electron transfer, these results suggest that ART antibacterial activity involves ROS generation under aerobic conditions.

The involvement of ROS in the ARS antibacterial activity prompted us to explore whether ARS bioactivity is associated with ROS-mediated DNA damage. Since DNA damage involving double-strand breaks (DSBs) can recruit the damage-inducible repair foci involving RecN [39], we have created a RecN-mClover3 fusion to visualize the ART-mediated DNA damage in VC cells. As shown in Figure 4(a and b), we found that RecN foci were formed by ART as well as H_2O_2 . These results suggest that ART could cause DNA damage in vivo, reminiscent of the effect of ROS.

ARS is bactericidal, which is enhanced by copper ion

The involvement of ROS in the ARS-mediated antibacterial killing indicates that ARS is bactericidal. To

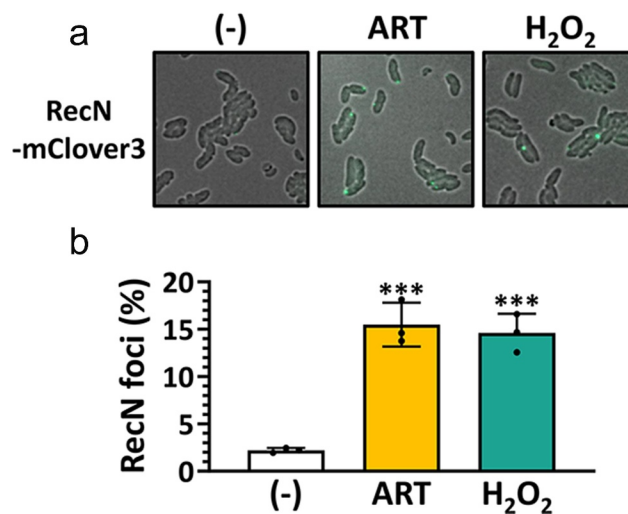


Figure 4. Enhancement of ARS-induced DNA damage in VC.

(A and B) Formation of DNA double-strand breaks (DSBs) by ART in vivo. The VC cells were treated with either ART (31.3 μ g/ml) and H_2O_2 (150 μ M) for 30 min. The DNA DSBs were monitored as the foci formation by RecN-mClover3, which was visualized by fluorescence microscope (A). The foci-positive cells in A were counted as the cells with DNA damage and the fractions of those with DNA damage were quantitated (B). Statistical significance between the groups is indicated, based on a *p* value of less than 0.001 (***) by Student's *t* test. The values are averaged from the three independent technical replicates and the error bars represent the standard deviations.

confirm its mode of action, we first performed time-to-kill assays and determined that ARS is bactericidal against VC (Figure S4). In this standard time-to-kill assay, more than a 3-log reduction in viability was observed by ARS treatment within 6 h.

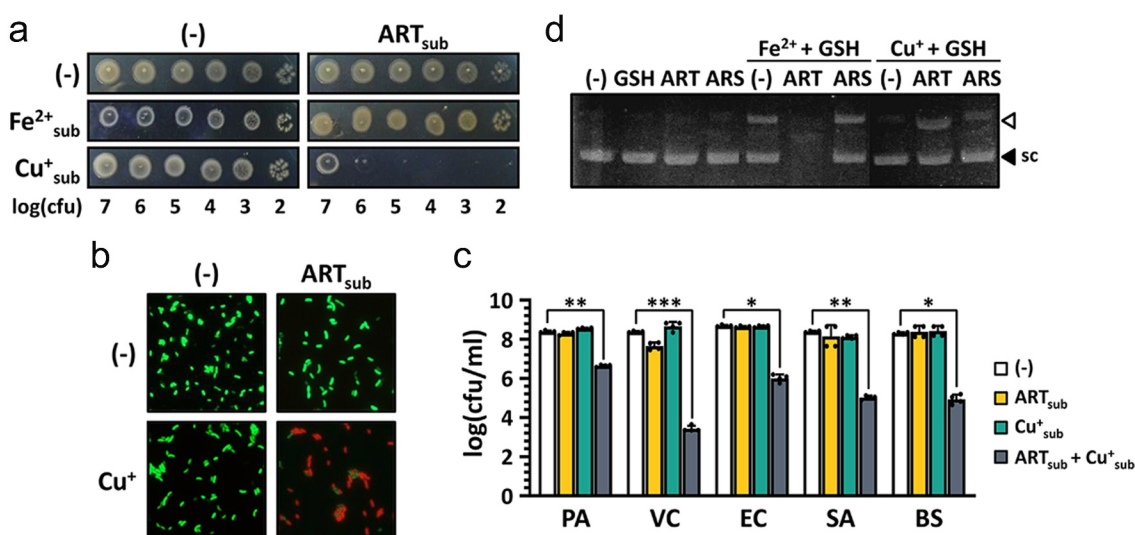


Figure 5. Enhanced antibacterial activity of ARS by copper addition.

(A) Effect of transition metal ions, Fe^{2+} or Cu^+ on the susceptibility of VC to the sub-inhibitory concentration (1.57 $\mu\text{g/ml}$) of ART (ART_{sub}). The VC cells were grown to the logarithmic growth phase. Ten-fold serial dilutions from the cell cultures were spotted onto an LB agar plate (-) and an LB agar plate with ART (ART_{sub}), which had been unsupplemented (-) or supplemented with 2.5 mM FeSO_4 (Fe^{2+} _{sub}), or 0.313 mM CuCl (Cu^+ _{sub}). The numbers indicate the log(cfu) of the applied bacterial spots. (B) Effect of Cu^+ on the pulse-treatment of ART in VC killing. The VC cells were grown to the logarithmic growth phase. The cells were pulse-treated with ART (31.3 $\mu\text{g/ml}$) and/or CuCl (0.25 mM). After treatment, the cells were stained using a mixture of SYTO9 and propidium iodide (PI) and visualized by fluorescence microscope. (C) Effect of Cu^+ on the susceptibility of bacterial species to the sublethal concentration of ART (ART_{sub}). The five bacterial (PA, VC, EC, SA, and BS) cells (5×10^5 cfu/ml) were treated with the following: noting (empty); ART (yellow; ART_{sub}) at the sub-inhibitory concentrations (PA, 1.25 mg/ml; VC, 0.75 $\mu\text{g/ml}$; EC, 0.156 mg/ml; SA, 0.313 mg/ml; BS, 0.625 mg/ml); CuCl (green; Cu^+ _{sub}) at the sub-inhibitory concentrations (VC, 0.313 mM; PA, SA, and BS, 0.625 mM; EC, 1.25 mM); ART and CuCl (dark green; ART_{sub}+ Cu^+ _{sub}) at the indicated concentrations. The survivor cells were enumerated by viable cell counts. Statistical significance between the groups is indicated, based on a p value of less than 0.01 (*), 0.005 (**), or 0.001 (***) by Student's t test. (D) Strand break induction by ARS and ART in vitro. The supercoiled (sc) plasmid DNA samples were incubated for 20 min with ART (10 mM) or ARS (10 mM) in the presence of GSH (20 μM) and either FeSO_4 (10 μM) or CuCl (10 μM). Conversion of the sc DNA (filled arrow head) to either the open-circle (single-strand breaks) and/or to linear (double-strand breaks) forms (empty arrow head) was monitored by gel electrophoresis. Extensive double-strand breaks lead to DNA degradation. The control experiments with each component (GSH, ART, or ARS) were also performed.

Since ROS generation involves transition metal ions such as Fe^{2+} and Cu^+ [40] and, more importantly, the endoperoxide bridge of ARS is able to form an organic free radical by extracting an electron from Fe^{2+} of hemoglobin [15,41], we hypothesized that transition metal ions might play a crucial role in ARS bactericidal activity. To this end, we have examined whether the ART antibacterial activity was affected by supplementing Fe^{2+} and Cu^+ . It was found that the bacteria were killed even by ART at a sub-inhibitory concentration (1.57 $\mu\text{g/ml}$) in the presence of Cu^+ , but not Fe^{2+} , at their sub-inhibitory concentrations (0.313 mM for Cu^+ and 2.5 mM for Fe^{2+}) (Figure 5(a)). The Cu^+ -mediated enhancement of VC killing was also confirmed by 3-h pulse treatment with ART and Cu^+ at sub-inhibitory concentrations as shown in Figure 5b and S5. More importantly, Cu^+ addition significantly enhanced ART antibacterial activity against all the bacterial species tested, although bacteria other than VC were not affected at all by the ART treatment in the

absence of Cu^+ supplementation (Figures 2(d) and 5(c)). These results suggest that copper, rather than iron, may effectively act as a transition metal to generate carbon-centered ARS radicals by endoperoxide cleavage in VC.

To confirm the possibility of copper-mediated fission of ARS in vitro, we investigated whether DSBs were induced by ART in the presence of Cu^+ . As shown in Figure 5, DSBs of plasmid pUCP18 by ART were observed in the presence Cu^+ . It was found that the DSBs were further enhanced by ART in the presence of Fe^{2+} , although Fe^{2+} treatment itself was able to induce DSBs even in the absence of ART (Figure 5(d)). This might be due to the different in vitro reactivity between Fe^{2+} and Cu^+ under oxic conditions. The weaker activity of ARS than ART to induce DSBs might be accounted for by its poor aqueous solubility.

In order to further confirm the involvement of Cu^+ in ART antibacterial activity, VC cells that had been pretreated with either a Cu^+ -chelating agent, NC or

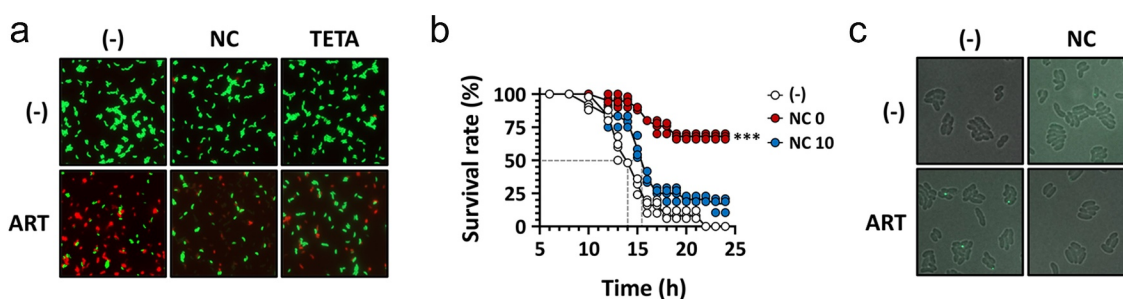


Figure 6. Reduced antibacterial activity of ARS by copper chelators.

(A) Effect of copper chelators on the ART-induced VC killing. The cells that had been grown to the logarithmic growth phase were treated with copper chelators, neocuproine (NC) (1.5 µM), or triethylenetetramine (TETA) (1.5 mM). After the chelator treatment, the cells were incubated with ART (313 µg/ml) for 1 h, stained as in Figure 3c and visualized by fluorescence microscope. (B) Effect of NC on the antibacterial efficacy of ART in *Drosophila* infections. Survival rates of VC-infected and ART-treated flies were determined upon NC. The flies were infected with VC cells that had been co-treated with ART (0.1 mg/ml) and NC at the indicated concentrations (0 or 10) (µM) and then transferred to new media. The survival was measured over time for the infected flies. The dotted lines represent the time required to reach 50% mortality. The statistical significance based on a log-rank test is indicated (***, $p < 0.001$). (C) Effect of copper chelators on the ART-induced DSBs. The VC cells were treated with NC (1.5 µM) and then incubated for 30 min on LB agarose pad with nothing (-) or ART (31.3 µg/ml). The DNA DSBs were monitored for the foci formation by RecN-mClover3, which was visualized by fluorescence microscope.

a Cu^{2+} -chelating agent, TETA were tested for their susceptibility to ART. As shown in Figure 6(a) and S6A, ART antibacterial activity was significantly reduced by both copper-depleting agents. It is surprising that TETA was also able to compromise ART activity. This is likely attributed to the interconversion between Cu^+ and Cu^{2+} in the cells, which could indirectly affect the Cu^+ level through Cu^{2+} depletion [42]. We also investigated whether or not NC could exert its inhibitory effect on ART antibacterial efficacy in *Drosophila* systemic infections. As shown in Figure 6 (b), the in vivo antibacterial efficacy of ART was also impaired by NC, suggesting that copper ions are critical to the ART antibacterial activity both in vitro and in vivo. Lastly, we examined whether the DNA damage has also been impaired by NC, in that ROS-mediated DNA damage might be responsible for the cell death under our experimental conditions. The formation of RecN-mediated foci was impaired by NC treatment (Figure 6(c) and S6B). These results indicate that copper ions are required for the ARS antibacterial activity against VC.

Discussion

To tackle the rapid emergence of AMR, multiple approaches have been developed to discover new antibacterials. Despite many efforts, new antibacterial discoveries still remain challenging, and alternative strategies; for example, combination therapies using antibacterial adjuvants are being proposed to solve the growing problem of AMR. Antibacterial adjuvants are considered to be

a promising therapeutic option that enhances bacterial susceptibility to treated antibacterials. These adjuvants improve antibacterial efficacy by compromising antibiotic resistance factors, enhancing antibiotic entry and accumulation, or stimulating the host immune responses [43].

In this study, we have shown that the antibacterial activity of the antimalarial ARS, which is enhanced by copper, was evidently revealed based on the first observation that VC is highly susceptible to ARS compared to other bacterial species. We have confirmed ARS antibacterial efficacy in vivo using *Drosophila* systemic infections caused by VC as well as other ESKAPE bacterial species, such as PA and SA. This suggests that copper might be more proficient under *Drosophila* infection conditions than under in vitro culture conditions where only VC displays ARS susceptibility. Further investigation regarding the quantitative assessment of copper in vivo will help address the difference between in vitro and in vivo antibacterial activity of ARS and thus provide the insight into clinical application of this information. In addition, considering the pharmacological properties of copper [44] as well as the IC_{50} values and the recommended initial dose of ARS as antimalarial monotherapy [45,46], the determined MIC values for VC would be considered as clinically achievable.

The involvement of copper in the ARS bioactivity can be ascribed to the catalytic decomposition of the ARS endoperoxide by copper and iron [14]. Interestingly, however, we found that the antibacterial activity of ARS was enhanced by addition of cuprous (Cu^+) ions but not by ferrous (Fe^{2+}) ions. It should be

noted that most of the studies have been focused on hemes and Fe^{2+} in regard to the antimalarial activity of ARS [12,21], most likely due to the scarcity of copper ions in bacterial cells, being one of the trace elements (at less than 100 μM) in biological systems [47]. Due to the potential toxicity of Cu^+ ions, bacteria tightly regulate cytoplasmic copper concentrations at a low level by a copper detoxifying/exporting system. It is still noteworthy that Cu^+ ions could enhance the toxic effect of ARS in bacterial cells. In the case of heme-copper oxidase, copper is preferred over iron in reducing oxygen to water because the redox potential of copper is lower than that of iron (+0.15 vs +0.77 V) [48]. Although it needs to be further verified whether or not the reactivity of ARS to each metal differs, it is presumable that Cu^+ ions could be a more biologically relevant contributor than Fe^{2+} ions in generating the ARS radicals in bacterial systems. This study highlights the therapeutic potential of this trace element as an adjuvant for ARS treatment of bacterial infections.

The selective antibacterial activity of ARS against VC was in part attributed to the higher intracellular level of copper in this bacterium under the ordinary in vitro culture conditions as shown in Figure S7. We hypothesized that this unique feature of VC might be associated with its natural habitats, where copper availability is highly limited [49]. This copper scarcity in the aquatic environment might also be associated with the lack of prominent copper efflux systems such as CusABC in VC [50], although the intracellular copper levels remain unclear in bacterial systems.

It is quite probable that the generated ARS organic radicals could react with the molecular oxygen (O_2) rather than directly with biological molecules. Thus, in the presence of O_2 , ROS can be formed by ARS radical-mediated electron transfer. The elevation of ARS-derived ROS generation is considered to induce cellular damage and death in a relatively nonspecific manner. ROS involvement in ARS bioactivity has been already suggested, in that the experiments had been performed under aerobic conditions, which is apparently relevant to the antimalarial action of ARS during the intraerythrocytic asexual reproduction cycle of the malaria parasite, *P. falciparum* [51]. Despite our finding that ARS is deemed ineffective under anaerobic conditions, the contribution of ROS generation is also evident in the antibacterial activity against VC. Alternatively, given that the colony morphologies of VC differ between aerobic and anaerobic conditions, it is likely that the physiomes regarding the factors affecting the susceptibility to ARS could differ between the two conditions. These might include the oxygen availability and, more importantly, copper availability

or others, which will be further elucidated by identifying the systems responding to resist copper toxicity in VC. ARS is also noteworthy because its antimalarial activity is evident at multiple life cycle stages of the parasite, in contrast to other antimalarials that are active only on a particular stage [52,53]. This promiscuous and potent activity of ARS is attributed to the ARS-derived radicals and/or their subsequent generation of ROS, which in turn could be translated into antibacterials in the presence of copper combination. Due to the potential toxicity caused by excessive copper accumulation, copper treatment in an appropriate dose range might be considered as a useful adjuvant [54,55]. This provides an insight into a combination therapy to repurpose an antimalarial to an antibacterial based on the micronutrient metal adjuvant and possibility of a common mechanism for the therapeutic activities of ARS. Therefore, further investigations of the phenotypic consequences that take place during the response to ARS in VC are likely to address unrevealed issues in the precise mechanisms of ARS bioactivity and, more importantly, resistance, further highlighting the utility and necessity of the tractable bacterial system.

Acknowledgments

This work was supported by the National Research Foundation of Korea (NRF) Grants (NRF-2017M3A9E4077205 and NRF-2017R1A2B3005239).

Author contributions

I.-Y.C. and Y.-H.C. conceived and designed the research. I.-Y.C. and H.-J.J. designed and performed the experiments, and collected and analyzed the experimental data. J.H., Y.-J. Y., H.-Y.O. and S.-H.K. provided reagents. I.-Y.C. and Y.-H.C. wrote the manuscript. All authors reviewed the manuscript.

Disclosure statement

No potential conflict of interest was reported by the author(s).

Data availability statement

The data that support the findings of this study are available from the corresponding author upon reasonable request (youhee@cha.ac.kr).

ORCID

You-Hee Cho  <http://orcid.org/0000-0001-7942-5893>

References

- [1] Prestinaci F, Pezzotti P, Pantosti A. Antimicrobial resistance: a global multifaceted phenomenon. *Pathog Glob Health*. 2015;109(7):309–318.
- [2] Payne DJ, Gwynn MN, Holmes DJ, et al. Drugs for bad bugs: confronting the challenges of antibacterial discovery. *Nat Rev Drug Discov*. 2007;6(1):29.
- [3] Tobinick EL. The value of drug repositioning in the current pharmaceutical market. *Drug News Perspect*. 2009;22(2):119–125.
- [4] Hien TT, White NJ. Qinghaosu. *Lancet*. 1993;341(8845):603–608.
- [5] Klayman DL. Qinghaosu (artemisinin): an antimalarial drug from China. *Science*. 1985;228(4703):1049–1055.
- [6] Medhi B, Patyar S, Rao RS, et al. Pharmacokinetic and toxicological profile of artemisinin compounds: an update. *Pharmacology*. 2009;84(6):323–332.
- [7] Efferth T, Kaina B. Toxicity of the antimalarial artemisinin and its derivatives. *Crit Rev Toxicol*. 2010;40(5):405–421.
- [8] Meshnick SR, Taylor TE, Kamchonwongpaisan S. Artemisinin and the antimalarial endoperoxides: from herbal remedy to targeted chemotherapy. *Microbiol Rev*. 1996;60(2):301–315.
- [9] Balint GA. Artemisinin and its derivatives: an important new class of antimalarial agents. *Pharmacol Ther*. 2001;90(2–3):261–265.
- [10] Haynes RK, Ho WY, Chan HW, et al. Highly antimalaria-active artemisinin derivatives: biological activity does not correlate with chemical reactivity. *Angew Chem Int Ed Engl*. 2004;43(11):1381–1385.
- [11] Antonie T, Fisher N, Amewu R, et al. Rapid kill of malaria parasites by artemisinin and semi-synthetic endoperoxides involves ROS-dependent depolarization of the membrane potential. *J Antimicrob Chemother*. 2014;69(7):1005–1006.
- [12] Meshnick SR, Yang YZ, Lima V, et al. Iron-dependent free radical generation from the antimalarial agent artemisinin (qinghaosu). *Antimicrob Agents Chemother*. 1993;37(5):1108–1114.
- [13] Klonis N, Crespo-Ortiz MP, Bottova I. Artemisinin activity against *Plasmodium falciparum* requires hemo-globin uptake and digestion. *Proc Natl Acad Sci USA*. 2011;108(28):11405–11410.
- [14] Garah F B-E, Pitie M, Vendier L, et al. Alkylating ability of artemisinin after Cu(I)-induced activation. *J Biol Inorg Chem*. 2009;14(4):601–610.
- [15] Li J, Zhou B. Biological actions of artemisinin: insights from medicinal chemistry studies. *Molecules*. 2010;15(3):1378–1397.
- [16] Ding XC, Beck HP, Raso G. *Plasmodium* sensitivity to artemisinins: magic bullets hit elusive targets. *Trends Parasitol*. 2011;27(2):73–81.
- [17] Meunier B, Robert A. Heme as trigger and target for trioxane-containing antimalarial drugs. *Acc Chem Res*. 2010;43(11):1444–1451.
- [18] Wang, J Zhang CJ, Chia WN, et al. Haem-activated promiscuous targeting of artemisinin in *Plasmodium falciparum*. *Nature Commun*. 2015;6(1):1–11.
- [19] Bhisutthibhan J, Pan XQ, Hossler PA, et al. The *Plasmodium falciparum* translationally controlled tumor protein homolog and its reaction with the anti-malarial drug artemisinin. *J Biol Chem*. 1998;273(26):16192–16198.
- [20] Eckstein-Ludwig U, Webb RJ, Van Goethem ID, et al. Artemisinins target the SERCA of *Plasmodium falciparum*. *Nature*. 2003;424(6951):957–961.
- [21] O'Neill PM, Barton VE, Ward SA. The molecular mechanism of action of artemisinin—the debate continues. *Molecules*. 2010;15(3):1705–1721. 10.3390/molecules15031705.
- [22] Efferth T, Romero MR, Wolf DG, et al. The antiviral activities of artemisinin and artesunate. *Clin Infect Dis*. 2008;47(6):804–811.
- [23] Uckun FM, Saund S, Windlass H, et al. Repurposing Anti-Malaria phytochemistry artemisinin as a COVID-19 drug. *Front Pharmacol*. 2021;12:407.
- [24] Galal AM, Ross SA, Jacob M, et al. Antifungal activity of artemisinin derivatives. *J Nat Prod*. 2005;68(8):1274–1276.
- [25] Ho WE, Peh HY, Chan TK, et al. Artemisinins: pharmacological actions beyond anti-malarial. *Pharmacol Ther*. 2014;142(1):126–139.
- [26] Wu Y, Zeng Q, Qi Z, et al. Recent progresses in cancer nanotherapeutics design using artemisinins as free radical precursors. *Front Chem*. 2020;8:472.
- [27] Lin L, Mao X, Sun Y, et al. Antibacterial mechanism of artemisinin/beta-cyclodextrins against methicillin-resistant *Staphylococcus aureus* (MRSA). *Microb Pathog*. 2018;118:66–73.
- [28] Gopalakrishnan AM, Kumar N. Antimalarial action of artesunate involves DNA damage mediated by reactive oxygen species. *Antimicrob Agents Chemother*. 2015;59(1):317–325.
- [29] Lee YJ, Jang HJ, Chung IY, et al. *Drosophila melanogaster* as a polymicrobial infection model for *Pseudomonas aeruginosa* and *Staphylococcus aureus*. *J Microbiol*. 2018;56(8):534–541.
- [30] Park SY, Heo YJ, Kim KS, et al. *Drosophila melanogaster* is susceptible to *Vibrio cholerae* infection. *Mol Cells*. 2005;20(3):409–415.
- [31] Kim BO, Jang HJ, Chung IY, et al. Nitrate respiration promotes polymyxin B resistance in *Pseudomonas aeruginosa*. *Antioxid Redox Signal*. 2021;34(6):442–451.
- [32] Park S, Imlay JA. High levels of intracellular cysteine promote oxidative DNA damage by driving the Fenton reaction. *J Bacteriol*. 2003;185(6):1942–1950.
- [33] Li W, Mo W, Shen D, et al. Yeast model uncovers dual roles of mitochondria in action of artemisinin. *PLoS Genet*. 2005;1(3):e36.
- [34] Jang HJ, Chung IY, Lim C, et al. Redirecting an anticancer to an antibacterial hit against methicillin-resistant *Staphylococcus aureus*. *Front Microbiol*. 2019;10:350.
- [35] Avery MA, Muraleedharan KM, Desai PV, et al. Structure-activity relationships of the antimalarial agent artemisinin. 8. design, synthesis, and CoMFA studies toward the development of artemisinin-based drugs against leishmaniasis and malaria. *J Med Chem*. 2003;46(20):4244–4258.
- [36] Hassett DJ, Alsabbagh E, Parvatiyar K, et al. A protease-resistant catalase, KatA, released upon cell lysis during stationary phase is essential for aerobic

- survival of a *Pseudomonas aeruginosa oxyR* mutant at low cell densities. *J Bacteriol.* **2000**;182(16):4557–4563.
- [37] Zimmermann A, Reimann C, Galimand M, et al. Anaerobic growth and cyanide synthesis of *Pseudomonas aeruginosa* depend on *anr*, a regulatory gene homologous with *fnr* of *Escherichia coli*. *Mol Microbiol.* **1991**;5(6):1483–1490.
- [38] Shin DH, Choi YS, Cho YH. Unusual properties of catalase A (KatA) of *Pseudomonas aeruginosa* PA14 are associated with its biofilm peroxide resistance. *J Bacteriol.* **2008**;190(8):2663–2670.
- [39] Hong Y, Zeng J, Wang X, et al. Post-stress bacterial cell death mediated by reactive oxygen species. *Proc Natl Acad Sci USA.* **2019**;116(20):10064–10071.
- [40] Valko M, Morris H, Cronin M. Metals, toxicity and oxidative stress. *Curr Med Chem.* **2005**;12(10):1161–1208. 10.2174/0929867053764635.
- [41] Kim SY, Park C, Jang HJ, et al. Antibacterial strategies inspired by the oxidative stress and response networks. *J Microbiol.* **2019**;57(3):203–212.
- [42] Beswick PH, Hall GH, Hook AJ, et al. Copper toxicity: evidence for the conversion of cupric to cuprous copper in vivo under anaerobic conditions. *Chem Biol Interact.* **1976**;14(3–4):347–356.
- [43] Liu Y, Li R, Xiao X, et al. Antibiotic adjuvants: an alternative approach to overcome multi-drug resistant Gram-negative bacteria. *Crit Rev Microbiol.* **2019**;45(3):301–314.
- [44] Denoyer D, Pearson HB, Clatworthy SA, et al. Copper as a target for prostate cancer therapeutics: copper-ionophore pharmacology and altering systemic copper distribution. *Oncotarget.* **2016**;7(24):37064–37080. 10.18632/oncotarget.9245.
- [45] He Z, Chen L, You J, et al. In vitro interactions between antiretroviral protease inhibitors and artemisinin endoperoxides against *Plasmodium falciparum*. *Int J Antimicrob Agents.* **2010**;35(2):191–193.
- [46] White NJ. Pharmacokinetic and pharmacodynamic considerations in antimalarial dose optimization. *Antimicrob Agents Chemother.* **2013**;57(12):5792–5807.
- [47] Finney LA, O'Halloran TV. Transition metal speciation in the cell: insights from the chemistry of metal ion receptors. *Science.* **2003**;300(5621):931–936.
- [48] Bhagi-Damodaran A, Petrik I, Lu Y. Using biosynthetic models of heme-copper oxidase and nitric oxide reductase in myoglobin to elucidate structural features responsible for enzymatic activities. *Isr J Chem.* **2016**;56:773–790.
- [49] Georgopoulos PG, Roy A, Yonone-Lioy MJ, et al. Environmental copper: its dynamics and human exposure issues. *J Toxicol Env Heal B.* **2001**;4(4):341–394.
- [50] Bondarczuk K, Piotrowska-Seget Z. Molecular basis of active copper resistance mechanisms in Gram-negative bacteria. *Cell Biol Toxicol.* **2013**;29(6):397–405.
- [51] Gunjan S, Sharma T, Yadav K, et al. Artemisinin derivatives and synthetic trioxane trigger apoptotic cell death in asexual stages of *Plasmodium*. *Front Cell Infect Microbiol.* **2018**;8:256.
- [52] Blasco B, Leroy D, Fidock DA. Antimalarial drug resistance: linking *Plasmodium falciparum* parasite biology to the clinic. *Nat Med.* **2017**;23(8):917.
- [53] Suresh N, Haldar K. Mechanisms of artemisinin resistance in *Plasmodium falciparum* malaria. *Curr Opin Pharmacol.* **2018**;42:46–54.
- [54] Gaetke LM, Chow CK. Copper toxicity, oxidative stress, and antioxidant nutrients. *Toxicology.* **2003**;189(1–2):147–163.
- [55] Szymański P, Frączek T, Markowicz M, et al. Development of copper based drugs, radiopharmaceuticals and medical materials. *Biometals.* **2012**;25(6):1089–1112.